Research Article
Vol. 25, No. 20 | 2 Oct 2017 | OPTICS EXPRESS 23684
Optics EXPRESS

Fabrication of high-temperature tilted fiber Bragg gratings using a femtosecond laser

Ruize Wang,[1] Jinhai Si,[1,2,*] Tao Chen,[1,2] Lihe Yan,[1,2] Houjun Cao,[1] Xuantung Pham,[1] and Xun Hou[1,2]

[1]*Key Laboratory for Physical Electronics and Devices of the Ministry of Education & Shaanxi Key Lab of Information Photonic Technique, School of Electronics & Information Engineering, Xi'an Jiaotong University, No. 28,Xianning West Road, Xi'an, 710049, China*
[2]*Xi'an Jiaotong University Suzhou Academy, Suzhou, 215123, China*
[*]*jinhaisi@mail.xjtu.edu.cn*

Abstract: We developed a new method to fabricate tilted fiber Bragg gratings (TFBGs) by using a femtosecond laser with a phase mask. During the laser processing, the fiber was obliquely moved at a tilt angle, in which the laser beam and the phase mask were fixed. The peak loss of the cladding modes with a tilt angle of 4.9° reaches to ~-8 dB, and the insertion loss is less than –0.2 dB. The TFBG was stable at temperature up to 700°C and slight degraded at 800 °C. The temperature sensing of the TFBG was demonstrated at a high temperature up to 800°C. The temperature sensitivities of the Bragg mode, the ghost mode, and the cladding mode were measured to be 15.72 pm/°C, 15.56 pm/°C, and 15.52 pm/°C, respectively. The refractive index response of the TFBGs was also measured.

OCIS codes: (060.3735) Fiber Bragg gratings; (060.2370) Fiber optics sensors; (140.7090) Ultrafast lasers.

References and links

1. N. J. Alberto, C. A. Marques, J. L. Pinto, and R. N. Nogueira, "Three-parameter optical fiber sensor based on a tilted fiber Bragg grating," Appl. Opt. **49**(31), 6085–6091 (2010).
2. X. Chen, J. Xu, X. Zhang, T. Guo, and B. O. Guan, "Wide Range Refractive Index Measurement Using a Multi-Angle Tilted Fiber Bragg Grating," IEEE Photonics Technol. Lett. **29**(9), 719–722 (2017).
3. G. Laffont and P. Ferdinand, "Tilted short-period fibre-Bragg-grating-induced coupling to cladding modes for accurate refractometry," Meas. Sci. Technol. **12**(7), 765–770 (2001).
4. S. C. Kang, S. Y. Kim, B. L. Sang, and S. W. Kwon, "Temperature-independent strain sensor system using a tilted fiber Bragg grating demodulator," IEEE Photonics Technol. Lett. **10**(10), 1461–1463 (1998).
5. C. F. Chan, C. Chen, A. Jafari, A. Laronche, D. J. Thomson, and J. Albert, "Optical fiber refractometer using narrowband cladding-mode resonance shifts," Appl. Opt. **46**(7), 1142–1149 (2007).
6. J. Albert, L. Y. Shao, and C. Caucheteur, "Tilted fiber Bragg grating sensors," Laser Photonics Rev. **7**(1), 83–108 (2013).
7. C. Chen, C. Caucheteur, P. Mégret, and J. Albert, "The sensitivity characteristics of tilted fibre Bragg grating sensors with different cladding thicknesses," Meas. Sci. Technol. **18**(10), 3117–3122 (2007).
8. C. Chen, Y. S. Yu, R. Yang, C. Wang, J. C. Guo, Y. Xue, Q. D. Chen, and H. B. Sun, "Reflective optical fiber sensors based on tilted fiber Bragg gratings fabricated with femtosecond laser," J. Lightwave Technol. **31**(3), 455–460 (2013).
9. E. Chehura, S. W. James, and R. P. Tatam, "Temperature and strain discrimination using a single tilted fibre Bragg grating," Opt. Commun. **275**(2), 344–347 (2007).
10. A. Kameyama, M. Katto, and A. Yokotani, "A simplified fabrication technique for tilted fiber Bragg grating for the simultaneous measurement of refractive index and temperature of liquids," J. Laser Micro Nanoeng. **9**(3), 230–233 (2014).
11. C. W. Smelser, D. Grobnic, and S. J. Mihailov, "Generation of pure two-beam interference grating structures in an optical fiber with a femtosecond infrared source and a phase mask," Opt. Lett. **29**(15), 1730–1732 (2004).
12. S. J. Mihailov, C. W. Smelser, D. Grobnic, R. B. Walker, P. Lu, H. Ding, and J. Unruh, "Bragg gratings written in all-SiO2 and Ge-doped core fibers with 800-nm femtosecond radiation and a phase mask," J. Lightwave Technol. **22**(1), 94–100 (2004).
13. D. Grobnic, C. W. Smelser, S. J. Mihailov, R. B. Walker, and P. Lu, "Fiber Bragg gratings with suppressed cladding modes made in SMF-28 with a femtosecond IR laser and a phase mask," IEEE Photonics Technol. Lett. **16**(8), 1864–1866 (2004).
14. M. L. Åslund, J. Canning, M. Stevenson, and K. Cook, "Thermal stabilization of Type I fiber Bragg gratings for operation up to 600°C," Opt. Lett. **35**(4), 586–588 (2010).

#304106
https://doi.org/10.1364/OE.25.023684
Journal © 2017
Received 4 Aug 2017; revised 6 Sep 2017; accepted 7 Sep 2017; published 18 Sep 2017

15. S. J. Mihailov, D. Grobnic, C. W. Smelser, P. Lu, R. B. Walker, and H. Ding, "Induced Bragg gratings in optical fibers and waveguides using ultrafast infrared laser and a phase mask," Laser Chem. **2008**, 416251 (2008).
16. W. Cui, T. Chen, J. Si, F. Chen, and X. Hou, "Femtosecond laser processing of fiber Bragg gratings with photo-induced gradient-index assisted focusing," J. Micromech. Microeng. **24**(7), 075015 (2014).
17. H. Chikh-Bled, K. Chah, Á. González-Vila, B. Lasri, and C. Caucheteur, "Behavior of femtosecond laser-induced eccentric fiber Bragg gratings at very high temperatures," Opt. Lett. **41**(17), 4048–4051 (2016).
18. Y. Li, C. R. Liao, D. N. Wang, T. Sun, and K. T. V. Grattan, "Study of spectral and annealing properties of fiber Bragg gratings written in H2-free and H2- loaded fibers by use of femtosecond laser pulses," Opt. Express **16**(26), 21239–21247 (2008).
19. C. Mou, K. Zhou, L. Zhang, and I. Bennion, "Characterization of 45°-tilted fiber grating and its polarization function in fiber ring laser," J. Opt. Soc. Am. B **26**(10), 1905–1911 (2009).
20. K. Markowski and P. Gąsior, "Inscription of the fibre Bragg gratings with femtosecond lasers," Proc. SPIE **9290**, 885–892 (2014).
21. C. Chen, L. Xiong, A. Jafari, and J. Albert, "Differential sensitivity characteristics of tilted fiber Bragg grating sensors," Proc. SPIE **6004**, 60040B (2005).

1. Introduction

Recently, tilted fiber Bragg gratings (TFBGs) have been broadly applied in the field of optical fiber sensors [1–6]. Because TFBGs have the dual sensing characteristics of uniform fiber Bragg gratings (FBGs) and long period fiber gratings (LPFGs) [3,7], they are suitable for temperature, strain and refractive index measurements [1,8,9]. To fabricate TFBGs, the conventional method is using a continuous wave (CW) or nanosecond ultraviolet (UV) laser [10]. It requires the fibers which have intrinsic photosensitivity or to be hydrogen loaded [11–13]. These grating structures are easily erased over 400°C [14]. In recent years, femtosecond infrared (IR) laser has been reported as a promising tool for the fabrication of FBGs, including uniform FBGs [16], tilted FBGs [8] and eccentric FBGs [17]. Differing from CW or nanosecond UV laser processing, femtosecond IR laser processing can be used to fabricate grating structures in various optical fibers resulting from the strong non-linear interaction between laser and materials [15]. In addition, FBGs fabricated with a femtosecond laser show better thermal stability, which can be used at high temperature even above 1000°C [18].

Up to now, the proposed method to fabricate TFBGs is to tilt the fiber at a tilt angle relative to the incident light and then inscribe a settled range with laser [2,3]. Because the incident direction of the laser is not perpendicular to the fiber core, the titled incident angle is different from the tilt angle of TFBG in the fiber, which increases the fabrication complexity [19]. Furthermore, the Bragg wavelength will be different for the TFBGs fabricated at different tilt angles because the periods of the TFBGs are dependent on the tilt angles. When a femtosecond laser is used to inscribe FBGs in fibers, the formation of FBGs in the fibers is mainly due to nonlinear optical effects, in which a small focal-length cylindrical lens is usually applied. The tilt angle of the fiber with respect to the phase mask becomes more rigors. When the focal line and the fiber are not parallel, it will lead to a complex condition inside the fiber, such as a distorted gratings structure, different focus positions with respect to the fiber core along the fiber axial direction, and TFBG structures extending to the fiber cladding [8]. Therefore, the transmission spectra of the TFBGs fabricated with this method present a lower peak loss and a higher insertion loss than that of TFBGs fabricated with a nanosecond UV laser.

In this paper, we demonstrated a new method to fabricate TFBGs by obliquely scanning. TFBG structures were formed using femtosecond laser irradiation and a phase mask. The tilt angle was introduced by obliquely moving fiber in the focal plane of cylindrical lens. In this method, 5-mm long TFBGs with different tilt angles were fabricated in a non-photosensitive SMF-28 fiber, and the grating structures only existed in the fiber core. The insertion loss is less than −0.2 dB. The peak loss of the cladding modes with the tilt angle of 4.9° reaches to about −8 dB. In addition, we investigated the effects of laser power and exposure time with TFBGs fabricated. Moreover, the temperature sensing of the TFBG using different modes were demonstrated at high temperature. The temperature sensitivities of Bragg mode, ghost

Optics EXPRESS

mode and cladding mode are 15.72 pm/°C, 15.56 pm/°C, and 15.52 pm/°C from 300°C to 800°C, respectively. The refractive index (RI) response of the TFBGs was also measured.

2. Experimental setup

The TFBG was fabricated in a single mode fiber (SMF-28). The diameter of fiber core is 9 μm. Grating structures were inscribed in fibers with femtosecond laser irradiation and a phase mask. The schematic of the TFBG fabrication system is shown in Fig. 1. Femtosecond laser pulses with a central wavelength of 800nm were generated by an amplified Ti:sapphire laser (Libra-USP-HE, Coherent Inc., USA) with 50-fs pulse duration and 1-kHz repetition rate. The 12-mm diameter Gaussian beam was focused with a cylindrical lens of focal length f = 25 mm through a zeroth-order-nulled phase mask with a pitch period Λ_m = 2.142 μm onto the fiber. According to free space Gaussian beam optics, the width of focal line is $W = 2\lambda f/\pi\omega_0$ = 2.1 μm, where λ is the laser wavelength, f is the focal length of the cylindrical lens, and ω_0 is the incident beam waist. To obtain pure two-beam interference gratings with a femtosecond pulse, the distance between fiber and phase mask was set to about 3 mm. Thus the diffracted beams of different order pairs (0, ± 1, ± 2, etc.) would not overlap resulting from an order walk-off effect [20]. The optical fiber was put on a piezoelectric platform (Thorlabs, NanoMax-TS, MAX302/M), fixed by magnetic fixtures. The platform can achieve three-dimensional translation with maximum lengths of 20 μm. Because the width of the focal line is less than the diameter of fiber core, we could make the FBG structures covering the fiber core by scanning fiber. A broadband ASE light source (Hoyatek, HY-ASE-C-13, with a spectra range of 1525-1570nm) and an optical spectrum analyzer (OSA) (Yokogawa, AQ6370D, with a spectral resolution of 20 pm) were used to measure the transmission spectra of TFBGs.

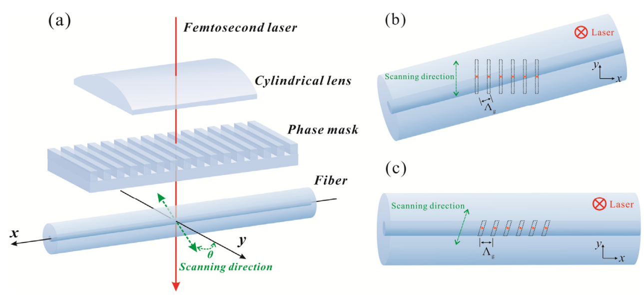

Fig. 1. (a) The schematic of fabricating TFBGs using femtosecond laser irradiation with a phase mask. (b) TFBGs fabricated by tilting the fiber. (c) TFBGs fabricated using our method.

The reported method of fabricating TFBGs with femtosecond laser and a phase mask is shown in Fig. 1(b). TFBGs were fabricated by tilting the fiber relative to x axis in x-y plane, and moving the fiber along the y axis to construct grating planes. We can see that part of the grating structures may extend to cladding in this method. According to Fig. 1(b), the period of gratings along the fiber axial direction is given by $\Lambda_g = \Lambda/\cos\theta$, where $\Lambda = \Lambda_m/2$ is the interference pattern period along the x axis, and θ is the angle between the fiber axis and the x axis. For TFBGs, the Bragg wavelength λ_B can be expressed as $\lambda_B = 2n_{eff}\Lambda_g$ [21], where n_{eff} is the effective refractive index of the Bragg mode at λ_B. Therefore, the Bragg wavelength increased as the tilt angle increasing. We demonstrate a new method to construct TFBGs by obliquely moving fiber sample in the x-y plane, which is shown in Fig. 1(c). In this method, the fiber sample places along with the x axis. The obliquely moving of fiber was realized through controlling the x and y axes moving simultaneously by a program. The tilt angle is calculated by $\theta = \arctan l_x/l_y$, where l_x and l_y are the moving lengths of fiber sample with x and y axes, respectively. The grating period along the fiber axial direction is given by $\Lambda_g = \Lambda_m/2$. Hence, the Bragg wavelength will be the same for TFBGs fabricated at different tilt angles. The grating structures can be precisely written in fiber core by setting scanning region.

Optics EXPRESS

3. Results and discussions

3.1 Processing results of TFBGs

The moving range of the fiber along with the *y* axis was set at 8 μm to make the grating structures covering the fiber core completely. The moving range of *x* was set at different values to obtain TFBGs with different tilt angles. The optical microscopic images of fs-written TFBGs with different tilt angles are shown in Fig. 2. From Fig. 2, we can see that the grating periods of the TFBGs are 1.07 μm. The length of the grating region is measured to be about 5 mm.

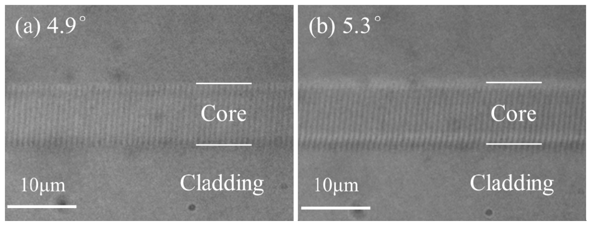

Fig. 2. Optical microscopic images of TFBGs fabricated at tilt angles of (a) 4.9° and (b) 5.3°.

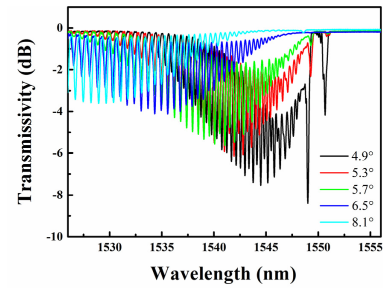

Fig. 3. The transmission spectra of the TFBGs with tilt angles of 4.9°, 5.3°, 5.7°, 6.5°, and 8.1°.

Figure 3 shows the transmission spectra of TFBGs with different tilt angles. As shown in Fig. 3, the resonance intensities of the Bragg mode and the ghost mode decrease as the tilt angel increasing. The peak loss of the cladding modes for the TFBG with a tilt angle of 4.9° reaches to about −8 dB, which decreases as the tilt angle increasing. The Bragg wavelengths are about 1550 nm for TFBGs with different tilt angles, which agree with our analysis above. The little difference of the Bragg wavelengths is because fibers are suffered from different strains when they are clamped by the fixtures during fabrication. In addition, we can see that the insertion loss is less than −0.2 dB.

The evolution of the transmission spectra with exposure time is shown in Fig. 4(a), in which the tilt angle and the laser power are set at 5.3° and 700 mW, respectively. From the inset of Fig. 4(a), we can see that the peak loss of the spectra of the TFBGs fabricated at laser power of 700 mW increases as exposure time increasing, and reaches to −6 dB at a saturation time of 50 s.

In addition, we investigated the influence of the laser power on the spectra of the fabricated TFBGs. Figure 4(b) shows the transmission spectra of TFBGs fabricated at laser powers of 500 mW, 600 mW, 700 mW and 800 mW, respectively. Table 1 shows peak losses of cladding modes and saturation times at different laser power.

From Fig. 4(b), we can see that the peak losses of the TFBGs fabricated at laser powers of 500 mW and 600 mW are only −0.9 dB and −3.4 dB, respectively. When the laser powers are set to 700 mW and 800 mW, the peak losses increase significantly and reach to about −6 dB. As shown in Tab. 1, the saturation time decreases as laser power increasing, and the saturation time decreases to about 50 s when the laser power is set at 700 mW. Because there are some breakages in the cladding for the TFBGs fabricated at a laser power of 800 mW, the optimal laser power to fabricate the TFBGs in our experiments is 700 mW.

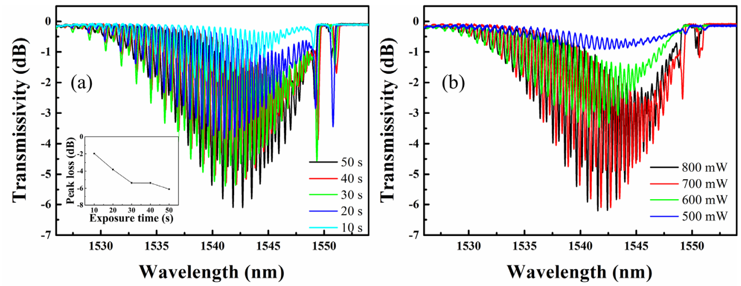

Fig. 4. The transmission spectra of the 5.3° TFBGs fabricated at (a) different exposure times and (b) different laser powers. The inset shows variations of peak loss as a function of exposure time.

Table 1. Peak losses and saturation times at different laser powers.

Laser power	500 mW	600 mW	700 mW	800 mW
Saturation time	270 s	120 s	50 s	40 s
Peak loss	-0.9 dB	-3.4 dB	-6.1 dB	-6.2 dB

As we known, besides SMF-28 fiber, FBGs have also been fabricated using femtosecond laser and phase mask in Yb^{3+} doped fiber, ZBLAN fiber, and so on [15]. Therefore, our proposed method could also be applied to fabricate in these kinds of fibers.

3.2 Thermal stability and temperature sensitivity

The fabricated TFBG was firstly annealed at 800 °C for 4 hours with a tube furnace and then used to study its thermal stability and temperature sensitivity. The sample was a TFBG with a tilt angle of 5.3°. After annealing treatment, the peak loss of the cladding modes decreased from −6 dB to −2.2 dB. It is because that some unstable grating structures were erased at high temperature of 800°C [14]. Then the tube furnace was set at 300°C, 400°C and 500°C for 30 min respectively to get stable spectra, and at 600°C, 700°C, and 800°C for 3 hours respectively to study the thermal stability. The Bragg mode, the ghost mode and the cladding mode at 1539.679 nm were monitored to study the temperature sensitivity of the TFBG. The results are shown in Fig. 5.

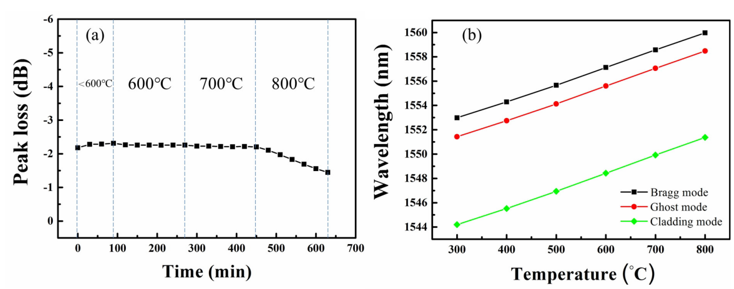

Fig. 5. (a) Evolution of the peak loss measured for the cladding mode at high temperatures. (b) Variations of the peak wavelength versus temperature measured for the Bragg mode, the ghost mode, and the cladding mode, respectively.

From Fig. 5(a), we can see that the peak loss of the cladding mode is stable up to 700°C, but decrease slowly at 800°C. As shown in Fig. 5(b), the peak wavelengths of the Bragg mode, the ghost mode, and the cladding mode increase with the temperature increasing. From linear fittings for each mode, the temperature sensitivities of the Bragg mode, the ghost mode, and the cladding mode are estimated to be 15.72 pm/°C, 15.56 pm/°C, and 15.52 pm/°C,

Optics EXPRESS

respectively. When Sapphire fibers are applied, the applicable temperature of the TFBG fabricated with our proposed method may be increased to above 1500°C [15].

3.3 RI response of TFBGs

In the RI sensing measurements, glycerin water solutions with different concentrations were used as the surrounding media and their refractive indexes were measured using an Abbe refractometer (Insmark, IR120). The TFBGs with the tilt angles of 5.3° and 8.1° were chosen to study their RI response. By changing the concentration of the glycerin water solution, the surrounding RI of was varied from 1.3324 to 1.4689 at 25°C. For the RI sensing measurements of the 5.3° and 8.1° TFBGs, we selected the cladding modes at the wavelengths of 1541.325 nm and 1528.472 nm, respectively, to monitor their peak wavelength shifts at different RI. The results are shown in Fig. 6.

From Fig. 6, we can see that the wavelength shift increase with refractive index increasing, and the RI sensitivity of the 8.1° TFBG is higher than that of the 5.3° TFBG. The wavelength shift for the 5.3° TFBG is about 0.4 nm with a RI range of 1.3324~1.4507.The wavelength shift for the 8.1° TFBG is about 0.5 nm with a RI range of 1.3324~1.4343. Its sensitivity is similar with that of the 7.3° TFBG fabricated with nanosecond UV laser [10]. The variations of the spectra of the 5.3° TFBG for different refractive index are shown in the inset of Fig. 6. We can see that the cladding modes at short wavelength side are gradually suppressed and the cladding response vanishes completely at the RI of 1.4689. For the 8.1° TFBG, the cladding response vanishes at the RI of 1.4416. Hence, the maximal measurable RI for the TFBG increased with the decrease of the tilt angle.

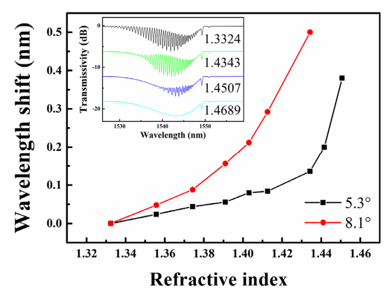

Fig. 6. Refractive index response of the TFBGs with the tilt angles of 5.3° and 8.1°. The inset shows variations of the spectrum of the 5.3° TFBG at different refractive indices.

4. Conclusion

We developed a new method to fabricate TFBGs by obliquely moving the fiber sample at a tilt angle. In this method, 5-mm long TFBGs with different tilt angles were fabricated in the non-photosensitive SMF-28 fiber, and the grating structures could be controlled to only exist in the fiber core. The insertion loss is less than −0.2 dB. The temperature sensitivities of the Bragg mode, the ghost mode, and the cladding mode are 15.72 pm/°C, 15.56 pm/°C, and 15.52 pm/°C, respectively. The refractive index response of the TFBGs was also measured.

Funding

The National Key Research and Development Program of China (2017YFB1104600); Suzhou Science and Technology Planning Project (SYG201622); Key Research and Development Program of Shaanxi Province; Program of the Collaborative Innovation Center of Suzhou Nano Science and Technology.